JOURNAL OF COMPUTATIONAL PHYSICS **145,** 432–444 (1998)
ARTICLE NO. CP986026

Fast Shallow-Water Equation Solvers in Latitude-Longitude Coordinates

William F. Spotz, Mark A. Taylor, and Paul N. Swarztrauber

National Center for Atmospheric Research, P.O. Box 3000, Boulder, Colorado 80307
E-mail: spotz@ucar.edu, taylorm@ucar.edu, and pauls@ucar.edu

Received March 3, 1998; revised May 15, 1998

Here we redirect attention to a fast pseudospectral method on the sphere developed by Merilees in 1973, recently revived by Fornberg. In these works, the required spatial derivatives are computed by the formal differentiation of one-dimensional Fourier series approximations to both scalar and vector functions on the surface of the sphere. Filters must be used to alleviate prohibitive time-stepping restrictions and maintain stability on the non-isotropic latitude-longitude grids. Merilees' original filter was eventually found to be unusable, as it was unstable for longer runs. In this paper we examine alternatives to Merilees' filter. In particular, we first use a harmonic filter that consists of a harmonic analysis followed directly by a synthesis. The resulting stability and accuracy are identical to the traditional spectral transform method. Fewer Legendre transforms are required since they are limited to the filter and not used to compute spatial derivatives. In theory, this approach can also be viewed as a fast spectral method since fast harmonic filters exist in the literature. Next we examine alternative fast Fourier filters with intent to reproduce the accuracy and stability provided by the harmonic filter. Computational examples are provided with both high order difference and Fourier derivative calculations. In addition, results are presented for both harmonic and Fourier filters.

1. INTRODUCTION

Many current state-of-the art global atmosphere models, such as a majority of those in the Atmospheric Model Intercomparison Project [5], utilize the spectral transform method (STM). This class of methods, comprehensively reviewed in [20], provides an elegant solution to the pole problems induced by a spherical coordinate system. Waves are uniformly resolved at all points on the sphere including the poles, and the resulting stability and accuracy have made it the method of choice for most models. The major drawbacks of the method are its computational cost and communication overhead on distributed memory computer architectures. Here, we address the first concern in the context of an explicit

0021-9991/98 $25.00

Eulerian method. If N represents the number of grid points in the latitude direction, the STM (or more specifically, the associated Legendre transforms) requires $\mathcal{O}(N^3)$ operations, which is larger than any other computation in weather modeling by a factor of N. At the time the STM rose in popularity, it was competitive at the resolutions contemporary computing architectures could handle, and for smooth fields is still the cheapest method per digit of accuracy. However, to resolve certain small-scale atmospheric features, N has been increased to the point that the Legendre transforms require a significant portion of the overall computing time.

Since its adoption in global climate models, the hope has been that a fast Legendre transform [2, 11] would be found, perhaps analogous to the fast Fourier transform, that would provide computations in spherical geometry with the efficiency available in Cartesian geometry. More than 20 years have passed without significant practical progress toward this goal [3]. Here we develop a class of fast spherical shallow water equation solvers using methods that reduce or bypass the explicit computation of the Legendre transform. Our motivation is therefore to find a method which is more efficient in terms of operations than the STM, yet which does not compromise the accuracy and stability we currently enjoy. Our search has been guided by the following observations:

(1) Spherical harmonic basis functions provide an isotropic representation of scalar functions on the surface of the sphere. Grid-based isotropic representations are limited to the vertices of Platonic solids, the largest of which is the 20-vertex dodecahedron. Although unstructured grid methods (see, for example, [7, 8, 15, 18, 22, 23]) have shown promise, they are difficult to incorporate into existing weather codes because of the underlying grid structure. On the other hand, latitude-longitude grids, which are highly non-isotropic, have some advantages in terms of ease of storage and periodicity, but introduce a set of problems associated with the poles. For example, the grid spacing near the poles places an unacceptable restriction on the time step. For this reason, methods based on latitude-longitude grids use filtering to maintain stability. Filtering is also used to dealias the nonlinear terms.

(2) A number of fast methods for computing spatial derivatives on latitude-longitude grids already exist which have been largely ignored due to the popularity of the STM. These approaches warrant re-examination with new filters, in conjunction with lessons learned from our current models, and in the context of the now-standard shallow-water test suite [27]. These methods include the pseudospectral approach of Merilees [13, 12] (recently revived by Fornberg [4]) and the fourth-order compact approach of Gilliland [6] (based on the ideas of Hirsh [9]). Our findings strongly suggest that the difference between spectral and fourth-order accuracy is negligible for realistic problems if a suitable filter is applied.

(3) A nearly ideal filter exists. The spherical harmonic filter (SHF) is obtained if we transform the variables to spherical harmonic space and directly back to grid space thus projecting our approximations onto the space of spherical harmonic basis functions. Since a triangular truncation of spherical harmonics provides half as many basis functions as grid points (fewer if dealiasing is employed), this operation results in a truncation of high wave numbers near the poles. The SHF is not a fast algorithm in the sense of the FFT or finite difference operators. However, Jakob-Chien and Alpert [10] have recently published a fast multipole SHF (which was subsequently improved by Yarvin and Rokhlin [28]). Combined with a fast method for computing spatial derivatives, this implies the existence of a fast STM in the sense of a fast Fourier transform.

The paper is organized as follows: Section 2 covers the two spatial derivative methods studied, starting with the features common to both methods, followed by the details of the pseudospectral method and the fourth-order compact method. Section 3 demonstrates the accuracy and stability of these methods when used in conjunction with a slow version of the SHF. Section 4 covers the results of numerical experiments applying a fast Fourier truncation filter to the various methods for solving the standard test suite of model problems. Conclusions are drawn in Section 5.

2. NUMERICAL METHODS

To emphasize the importance of the spherical harmonic filter, we will apply it to two methods for computing fast and accurate derivatives on the sphere; namely, Merilees' pseudospectral method and the fourth-order compact differencing method. We start with the features that are common to both methods.

2.1. *Common Features*

Both numerical models solve the advective form of the shallow-water equations in spherical coordinates, given by

$$\frac{\partial \mathbf{v}}{\partial t} = -(\zeta + f)\boldsymbol{k} \times \mathbf{v} - \nabla\left(\frac{1}{2}\mathbf{v}\cdot\mathbf{v} + gH\right), \tag{1}$$

$$\frac{\partial h}{\partial t} = -\nabla \cdot (h\mathbf{v}), \tag{2}$$

where $\mathbf{v} = (u, v)$ is the spherical velocity vector and h is the atmospheric thickness. Thus, the height above sea level, $H = h + h_s$, where h_s is the height of the underlying mountains (note that in the standard test suite, only Case 5 includes topography, with a single isolated mountain). The vorticity ζ and Coriolis parameter f are given by

$$\zeta = \boldsymbol{k} \cdot \nabla \times \mathbf{v}, \tag{3}$$

$$f = 2\Omega \sin\theta, \tag{4}$$

where $\boldsymbol{k}$ is the outward unit vector normal to the surface of the sphere and Ω is the earth's rotation rate.

Each numerical method utilizes a latitude-longitude (θ, λ) grid with equal grid spacing $(\Delta\theta = \Delta\lambda)$. Furthermore, the latitude grid points are shifted a half-grid length such that the poles are *not* data points and the most extreme latitudes stored are at $\pm(\frac{\pi}{2} - \frac{\Delta\theta}{2})$. Thus the grid dimension is $N \times 2N$. A grid which contains points at the poles is of course also possible, but this requires developing a special formulation at the poles based on transforming the dynamics equations to Cartesian coordinates. By using the shifted latitude grid, the $1/\cos\theta$ term which appears as part of the spherical ∇-operators thus requires no special treatment at the poles. This feature also helps load-balance parallel implementations of the different methods.

Time-integration is accomplished by simple leap-frog with a stabilizing Robert filter [17]. The procedure is boot-strapped with a single Euler time step and a single leap-frog step at $\Delta t/2$. The values of Δt for the resolutions used in this study are presented in Table I. This

TABLE I
Time-Step Values for the Resolutions Studied

Grid	Resolution	Δt
T21	32×64	360 s
T42	64×128	180 s
T85	128×256	90 s

is an explicit procedure that uses the spatial derivatives only at the current time step. The two models differ only in how the spatial derivatives are approximated.

2.2. *Merilees' Pseudospectral Model*

Spatial derivatives in Merilees' pseudospectral model (abbreviated here as the FFT method), described in detail in [4, 12, 13], are computed from a one-dimensional FFT along a single line in the desired direction, formally differentiating the series, and transforming back. This is trivial in the longitudinal direction, since the function is periodic at every latitude. For latitude derivatives, a great circle meridian is formed by connecting the latitude data separated by an angular distance π in longitude (or N grid points). This is illustrated in Fig. 1. The resulting periodic domain can be differentiated in Fourier space and transformed back. Since data on the "back" side of the sphere is differentiated with respect to $-\theta$, the resulting values for scalar derivatives must be negated to obtain the latitudinal derivatives. Velocity data (u, v), however, changes sign across the poles, and thus the computed derivatives on the "back" side are not negated.

A single FFT in either direction requires $\mathcal{O}(N \log N)$ operations, so computing the derivatives in both directions on the surface of the sphere is an $\mathcal{O}(N^2 \log N)$ operation.

While Merilees obtained good results with this method, it was not widely adopted because of the superior stability of the STM. Our goal here is to redirect attention to Merilees'

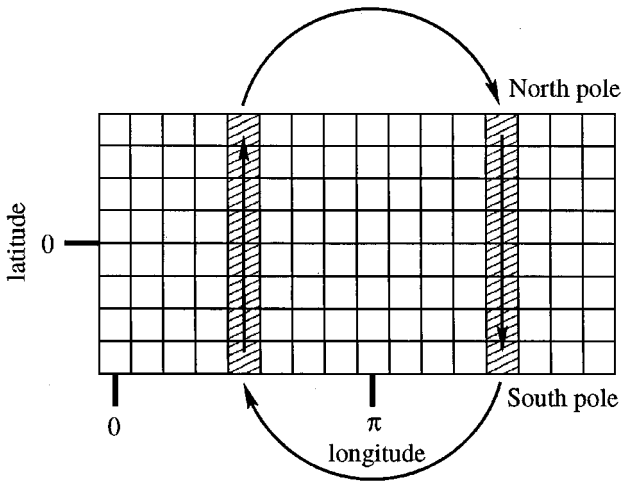

FIG. 1. Ordering of latitudinal data as a periodic domain. This requires the number of longitude points to be evenly divisible by two. Each box represents storage of a single data value at a grid point.

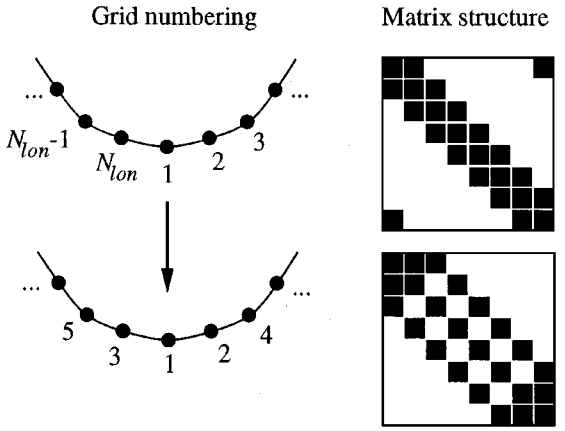

FIG. 2. Longitudinal grid number reordering used to change a near-tridiagonal periodic matrix into a strictly pentadiagonal matrix for the fourth-order compact model. The same principle is applied to the latitudinal grid numbering.

method by introducing alternate filters that more closely provide the accuracy and stability associated with the STM. The filters Merilees used will be discussed briefly in Section 4.

2.3. *Fourth-Order Compact Model*

Alternately, compactly supported fourth-order accurate (COM4) spatial derivatives can be computed using Hirsh's formula [9] (see also Gilliland [6]). For example, longitudinal derivatives of some generic transport variable ϕ are given by

$$\frac{1}{6}\frac{\partial \phi}{\partial \lambda}\bigg|_{i-1} + \frac{2}{3}\frac{\partial \phi}{\partial \lambda}\bigg|_{i} + \frac{1}{6}\frac{\partial \phi}{\partial \lambda}\bigg|_{i+1} = \frac{\phi_{i+1} - \phi_{i-1}}{2\Delta\lambda} + \mathcal{O}(\Delta\lambda)^4, \tag{5}$$

where we assume periodic indexing. Thus we must implicitly solve for all of the derivatives on a single line simultaneously. Direct application of (5) results in a nearly tridiagonal matrix with periodic boundary conditions. In practice, we renumber the indexes as shown in Fig. 2 to transform the matrix into a strictly pentadiagonal matrix. We then LU-decompose this new banded matrix once during initialization, reducing the actual derivative computations to a series of forward and backward elimination steps. This approach is slightly more expensive than other cyclic tridiagonal solvers [24], but is trivial to implement with existing banded matrix software packages. Regardless of the method chosen, computing all the derivatives in a single direction on the sphere is an $\mathcal{O}(N^2)$ operation. The grid renumbering is utilized only during the spatial derivative calculations.

Derivatives in the latitudinal direction are handled in the same manner, utilizing the technique described by Fig. 1 to create periodic meridional domains. By restricting $\Delta\lambda = \Delta\theta$, we can use the same LU-decomposed matrix that is used to compute longitudinal derivatives.

3. SPHERICAL HARMONIC FILTER

As noted in the Introduction, the spherical harmonic filter (SHF) is obtained by projecting the latitude-longitude data onto the space of spherical harmonics. This is equivalent to truncating certain waves such that the retained waves are isotropic on the sphere. This

method is faster than the standard STM because harmonic transforms are limited to the filter and not used to compute spatial derivatives. Filtering the scalar height field requires two transforms, and the most efficient vector transform (proposed by Swarztrauber [19], based on an algorithm by Temperton [25]) requires four transforms to filter the velocity, for a total of six transforms. Compare this to nine transforms for the most efficient STM [16] or an average of 13 transforms for most forms of the STM [20]; and speedups of 33–54% of the dynamical cores of atmospheric models are immediately possible.

We implemented this filter by using SPHEREPACK 2.0 [1]. Thus our implementation is $\mathcal{O}(N^3)$, although faster SHFs are available in the literature. For example, Jakob-Chien and Alpert [10] have developed a fast multipole spherical filter with accuracy that is comparable to the SHF which is $\mathcal{O}(N^2 \log N)$. Their algorithm has been improved by Yarvin and Rokhlin [28].

An important aspect of the spherical harmonic filter is that it produces exactly the same results as the equispaced STM (to within roundoff error) when combined with the pseudospectral method. Consider an arbitrary time level; the prognostic variables will be band-limited because they were just filtered at the previous time step. The pseudospectral derivatives in the longitude direction will therefore be exact, because spherical harmonics are simply Fourier series in the longitudinal direction. The same is true in the latitude direction, because the associated Legendre functions can be expressed as polynomials of trigonometric functions in latitude. This result is demonstrated in this and the following section.

We will first look at two test cases that are representative of smooth and non-smooth solutions. A more comprehensive table of results for all test cases is provided in Section 4. Figure 3 is a plot of the convergence of the L^2 error in h for the spherical harmonic filter applied to our two numerical methods for Case 3 in [27]. Test Case 3 is a smooth, steady state solution to (1) and (2). For a smooth solution, the difference in accuracy between the

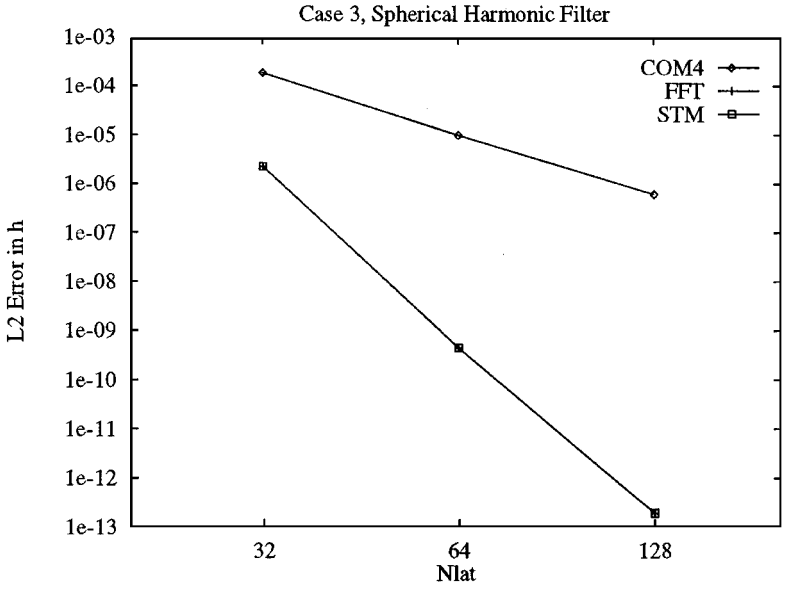

FIG. 3. Convergence of h for the spherical harmonic filter with respect to spatial resolution for Test Case 3, $\alpha = \pi/3$. COM4 is the fourth-order compact method, FFT is the pseudospectral method, and STM is the spectral transform method.

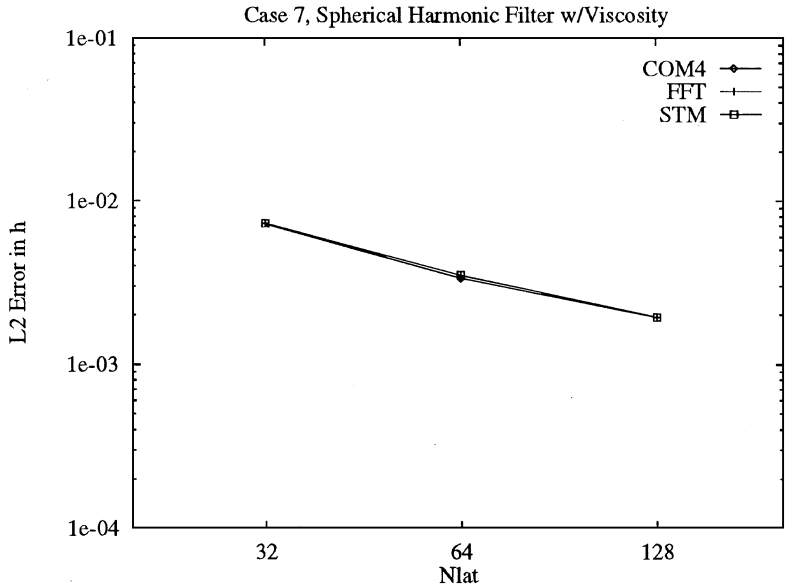

FIG. 4. Convergence of h for the spherical harmonic filter with respect to spatial resolution for Test Case 7, $u_0 = 20$. COM4 is the fourth-order compact method, FFT is the pseudospectral method, and STM is the spectral transform method.

fourth-order method and the pseudospectral method is apparent. Furthermore, we see that the STM and the FFT/SHF methods produce identical results. It should be noted that the STM used for comparison here was also on an equispaced latitude grid, but care was taken (as in the filter) to use a transform that is exact for band-limited functions [21].

Figure 4 is the same as Fig. 3 except that the results are for Case 7, which uses analyzed 500-mb height and wind field initial conditions from 0000 GMT December 21, 1978. These initial conditions were chosen because of the strong flow over the north pole. Results are compared to a highly refined spectral transform solution. The lack of smoothness in the solution results in a very slow rate of convergence for all of the methods, and it can be seen that the pseudospectral, fourth-order compact, and spectral transform methods all perform nearly identically for this "more realistic" model problem.

Remark. It should be noted that Test Case 7, as specified in [27], calls for the methods and reference solution to be obtained using explicit diffusion. This is required to maintain stability for a full-featured 3D climate model and so the shallow water test is designed to give an indication of how models would run in this setting. However, the STM does not require explicit diffusion to maintain stability for the shallow water equations. On the other hand, diffusion (or dealiasing) is required by the FFT and COM4 methods. As such, it is possible to improve the STM results in Fig. 4 by optimizing it for the shallow water equations.

Based on the results of these two test cases, we have demonstrated that the problem of finding a fast method with spectral transform properties can be reduced to finding a fast spherical harmonic filter, and such filters have recently appeared in the literature. Thus, in theory, we have a fast dynamical core for an atmospheric model which is just as accurate and stable as the STM, but faster by a factor $N/\log N$. However, even though fast multipole methods are $\mathcal{O}(N)$ for N data points, they are still relatively expensive for resolutions

common to atmospheric models. Therefore, it would still be to our advantage to find a fast filter based purely on FFTs. This is the topic of the following section.

4. THE FAST FOURIER TRUNCATION FILTER

The fast Fourier truncation filter (FTF) we employ is implemented by transforming the prognostic variables to Fourier space with one-dimensional FFTs in the specified direction, truncating undesired coefficients, and transforming back for each time step. As with the pseudospectral model, it requires $\mathcal{O}(N^2 \log N)$ operations. Two types of truncation are employed: polar truncation to alleviate the CFL condition, and dealiasing truncation to prevent the aliasing of nonlinear terms.

For the polar filter (see Umscheid and Sankar-Rao [26]), the truncated wave numbers m are those that satisfy the relation

$$m > N \cos\theta.$$

This filter is chosen such that the smallest retained wavelengths near the poles are roughly equal to the smallest equatorial wavelengths. Therefore the time step can be determined by the CFL condition at the equator thereby increasing the time step by a factor of N over an unfiltered model. Since the errors should be dominated by the smallest equatorial wavelengths, the accuracy should be effectively unchanged by the polar filter.

Merilees [13] applied the polar filter to his pseudospectral model at latitudes $|\theta| > 60^\circ$ to save on the number of required FFTs. We apply the polar filter everywhere since we also dealias everywhere and would not see the savings.

The well-known dealiasing filter truncates the top third of the spectrum to eliminate the effect of aliasing from nonlinear terms (see Orszag [14]). This is achieved by truncating wave numbers

$$m > \frac{2}{3}N, \tag{6}$$

which can be applied in both latitude and longitude directions. Merilees [13] truncated the wavelengths less than three grid lengths once every three hours. Dealiasing was applied in both the latitude and longitude directions, for both the pseudospectral method and the fourth-order compact method.

In the longitude direction, the dealiasing filter can be combined with the polar filter in at least two different ways. First, by truncating

$$m > N \min\left(\cos\theta, \frac{2}{3}\right), \tag{7}$$

in which the crossover between filters occurs at approximately $\theta = \pm 48^\circ$. Or second, by truncating

$$m > \frac{2}{3}N\cos\theta. \tag{8}$$

The first combination, relationship (7), is equivalent to applying the polar filter first and then dealiasing. The second combination, relationship (8), is equivalent to dealiasing first and then applying the polar filter such that the smallest retained wavelength is equal to the smallest *retained* equatorial wavelength. This constitutes more filtering than (7), and thus

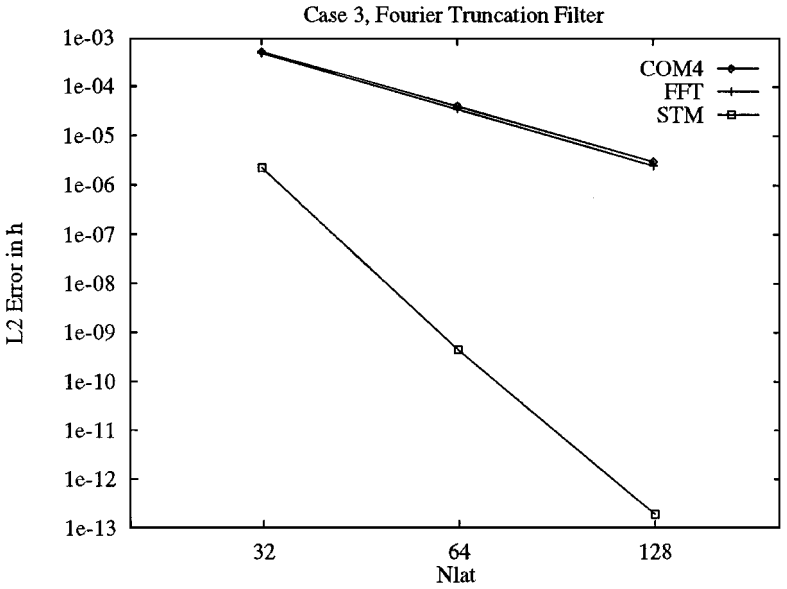

FIG. 5. Convergence of h for the Fourier truncation filter with respect to spatial resolution for Test Case 3, $\alpha = \pi/3$. COM4 is the fourth-order compact method, FFT is the pseudospectral method, and STM is the spectral transform method.

represents a somewhat less accurate method. We therefore used the min relationship (7) in our numerical experiments.

Figure 5 is the same as Fig. 3 except that the results are for the Fourier truncation filter. For this smooth problem, the pseudospectral method loses accuracy relative to the STM and the SHF. But the accuracy is still acceptable, and is quite close to the fourth-order compact results.

Figure 6 is the same as Fig. 4 except that the results are again for the Fourier truncation filter. For this non-smooth "realistic" problem, the results for the various methods do not significantly differ. Note that, as in Fig. 4, the errors are relatively large and the slopes of the lines represent roughly first-order convergence. This indicates that the mesh size is not yet in the asymptotic realm. This is typical convergence behavior for realistic atmospheric problems.

Remark. Given the superior accuracy of the STM for Case 3, it may be of some concern that the COM4 and FFT methods yield more accurate results than the STM for Case 7. We believe this behavior can perhaps be related to how dealiasing is implemented for the different filters. Because a triangular truncation is utilized for the STM (and the SHF), the two-thirds rule results in retaining only 44% of all possible wave modes. For the FTF, the percentage of retained waves in the latitude direction, by using (6), is 67%, and in the longitude direction, by using (7), is roughly 52%. Thus we claim the two-thirds rule, as implemented in the FTF, retains more modes and thus more accuracy than the SHF. Indeed, the accuracy of the SHF can be made to exceed that of the FTF by increasing the number of retained modes. In fact, as noted before, the STM can be run without any dealiasing at all, but the COM4 and FFT methods require it. Clearly, this behavior requires further study.

Table II gives the normalized L^2 error in h for all seven test cases solved with the spectral transform method and the four combinations of the spherical harmonic and Fourier

TABLE II
Test Case Results

Method	Grid	Normalized L^2 error in h						
		Case 1	Case 2	Case 3	Case 4	Case 5	Case 6	Case 7a
STM	T21	0.042	1×10^{-13}	2×10^{-6}	0.39	0.0019	0.014	0.0073
	T42	0.011	2×10^{-13}	4×10^{-10}	0.00082	0.00096	0.0044	0.0035
	T85	0.0050	3×10^{-13}	2×10^{-13}	0.00040	0.00077	0.0011	0.0019
FFT/SHF	T21	0.042	1×10^{-13}	2×10^{-6}	0.39	0.0019	0.014	0.0073
	T42	0.011	2×10^{-13}	4×10^{-10}	0.00082	0.00096	0.0044	0.0035
	T85	0.0050	3×10^{-13}	2×10^{-13}	0.00040	0.00077	0.0011	0.0019
COM4/SHF	T21	0.27	1×10^{-6}	2×10^{-4}	0.38	0.0023	0.015	0.0072
	T42	0.042	8×10^{-8}	1×10^{-5}	0.013	0.00096	0.0046	0.0034
	T85	0.0094	5×10^{-9}	6×10^{-7}	0.00059	0.00077	0.0012	0.0019
FFT/FTF	T21	0.053	2×10^{-14}	5×10^{-4}	0.23	0.0018	0.034	0.0057
	T42	0.012	8×10^{-14}	3×10^{-5}	0.00084	0.00091	0.011	0.0035
	T85	0.0051	2×10^{-13}	2×10^{-6}	0.00042	0.00076	0.0045	0.0013
COM4/FTF	T21	0.27	1×10^{-6}	5×10^{-4}	0.28	0.0052	0.034	0.0057
	T42	0.042	8×10^{-8}	4×10^{-5}	0.028	0.00091	0.011	0.0035
	T85	0.0094	5×10^{-9}	3×10^{-6}	0.0023	0.00093	0.0045	0.0014

Note. Standard shallow water test case results for the pseudospectral method (FFT) and fourth-order compact method (COM4) in conjunction with the spherical harmonic filter (SHF) and the Fourier truncation filter (FFT). The spectral transform method (STM) is included for reference.

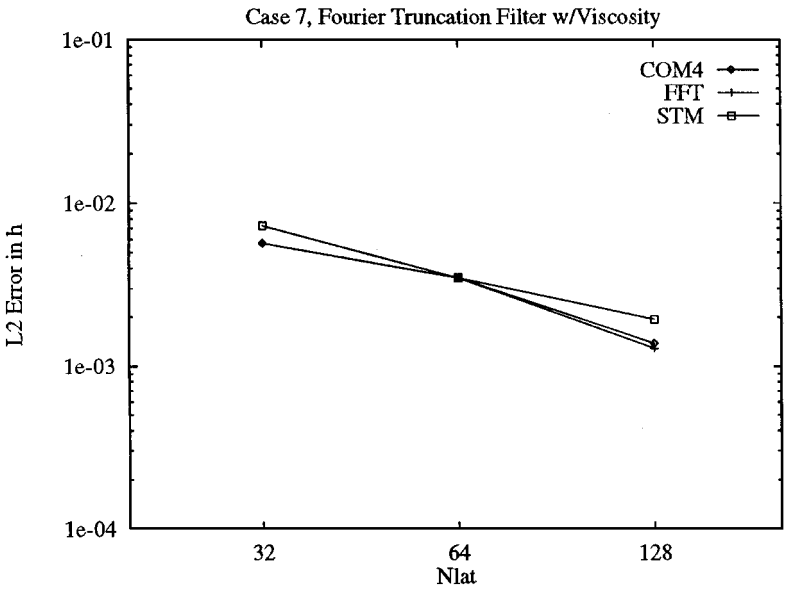

FIG. 6. Convergence of h for the Fourier truncation filter with respect to spatial resolution for Test Case 7, $u_0 = 20$. COM4 is the fourth-order compact method, FFT is the pseudospectral method, and STM is the spectral transform method.

truncation filters used with the pseudospectral and fourth-order compact methods. The problem duration and error norm specification are as required by [27]. We used the same explicit time step we would normally use in a full global climate model, as reported in Table I. This sometimes led to dominant time-step truncation errors, as reported below. Note that for all cases at all grid resolutions the solutions for STM and FFT/SHF are identical to the reported number of digits.

Test Case 1 is pure linear advection of a cosine bell around the sphere, in this case, directly over the poles ($\alpha = \pi/2$, where α is the angle of solid body rotation). The cosine bell is discontinuous in the second derivative and this restricts the accuracy of any method which does not specifically compensate for this fact, such as an adaptive grid approach. Nevertheless, the pseudospectral method is more accurate than the fourth-order differencing method. Note that COM4 is identical for either filter used. Therefore the truncation error is the dominant source of error for this method applied to this test case.

Test Case 2 is a steady-state solution for global nonlinear zonal geostrophic flow. We ran it for the case $\alpha = \pi/4$. The STM and pseudospectral methods are extremely accurate for this case, as the reported errors are clearly roundoff. COM4 is again identical for the two filters, indicating that the (still extremely small) error we observe is due to finite difference truncation.

Test Case 3 is similar to Test Case 2 except that the wind field is nonzero only in a limited region. We ran it with $\alpha = \pi/3$. Clearly, we are no longer seeing roundoff error, but the errors are still extremely small. These results are also plotted in Figs. 3 and 5.

Test Case 4 is a forced nonlinear system with translating low run with velocity parameter $u_0 = 20$. The forcing results in a higher sensitivity to time truncation errors and this effect is seen in the results. Note that the FFT method is virtually identical for the two filters at the higher resolutions and that the rate of convergence here drops off considerably. This is a time-stepping effect.

Test Case 5 is zonal flow over an isolated mountain. This case has a limit on accuracy because the zonal flow initial condition is not in geostrophic equilibrium with the topography, resulting in relatively significant gravity waves. These gravity waves are poorly resolved by the semi-implicit reference solution, and so the computed L^2 error for h for any method has an uncertainty of roughly 10^{-3} [23], which is reached by all methods by T42. However, it should be noted that the COM4/FTF combination required reducing the time step from 90 to 72 for grid T85 in order to converge. This indicates that the FTF is not as stable as the SHF, when combined with fourth-order compact differencing.

Test Case 6 is the Rossby–Haurwitz wave. This case calls for explicit diffusion. A damping time of 60 minutes was used for the SHF and a damping time of 240 minutes was used for the FTF, as these settings produced the most accurate results.

Test Case 7 is an analyzed 500-mb height and wind field initial conditions. The details of this case have been previously discussed and results for this case are also plotted in Figs. 4 and 6. The explicit diffusion is the same as in Test Case 6.

5. CONCLUSIONS

The experimental results presented here demonstrate that fast methods for computing spatial derivatives on the sphere used in conjunction with the spherical harmonic filter can produce results comparable to the spectral transform method in terms of accuracy

and stability. In fact, Merilees' method for computing spatial derivatives combined with the spherical harmonic filter produces results identical to the spectral transform method. The filter approach, however, requires only six of the computationally expensive Legendre transforms, down from nine transforms for Ritchie's method or an average of 13 transforms for other spectral transform approaches. Moreover, recent research suggests that even greater efficiency in the filter can be obtained with multipole algorithms.

In addition to the spherical harmonic-based filter, we also studied the behavior of a parameter-free FFT-based filter. The results of this approach in terms of accuracy are very close to STM results for realistic test cases, although some loss of accuracy can be observed for smooth test cases. This filter appears to be not quite as stable as the SHF for certain cases. Nevertheless, the overall results for this filter are very encouraging, and its speed and potential to mimic the spherical harmonic filter make it an obvious candidate for further study.

We have shown that the harmonic filter can be used to speed computations for an Eulerian model with explicit time stepping. It remains to be shown its affect in other models.

ACKNOWLEDGMENTS

This research was supported in part by the Advanced Studies Program at the National Center for Atmospheric Research; and the U.S. Department of Energy, Office of Energy Research, Special Research Grant: CHAMMP, Grant DE-FG05-91-ER61219.

REFERENCES

1. J. C. Adams and P. N. Swarztrauber, *Spherepack 2.0: A Model Development Facility*, Technical Report TN-436-STR, NCAR, Boulder, CO, September 1997.
2. J. Driscoll and D. Healy, Computing Fourier transforms and convolutions on the 2-sphere, *Adv. in Appl. Math.* **15**, 202 (1994).
3. European Center for Medium-Range Weather Forecasts, *Techniques for Horizontal Discretization in Numerical Weather Prediction Models*, November 2–4, 1987, 1988.
4. B. Fornberg, A pseudospectral approach for polar and spherical geometries, *SIAM J. Sci. Comput.* **16**(5), 1071 (1995).
5. W. L. Gates, AMIP: The atmospheric model intercomparison project, *Bull. Amer. Meteorological Soc.* **73**(12), (1992).
6. R. L. Gilliland, Solutions of the shallow water equations on the sphere, *J. Comput. Phys.* **43**(1), 79 (1981).
7. R. Heikes and D. A. Randall, Numerical integration of the shallow-water equations on a twisted icosahedral grid. Part I. Basic design and results of tests, *Monthly Weather Rev.* **123**, 1862 (1995).
8. R. Heikes and D. A. Randall, Numerical integration of the shallow-water equations on a twisted icosahedral grid. Part II. A detailed description of the grid and an analysis of numerical accuracy, *Monthly Weather Rev.* **123**(6), 1881 (1995).
9. R. S. Hirsh, Higher order accurate difference solution of fluid mechanics problems by a compact differencing technique, *J. Comput. Phys.* **9**(1), 90 (1975).
10. R. Jakob-Chien and B. K. Alpert, A fast spherical filter with uniform resolution, *J. Comput. Phys.* **136**, 580 (1997).
11. D. M. Healy, Jr., D. N. Rockmore, and S. B. Moore, An FFT for the 2-sphere and applications, in *Proceedings ICASSP 96, Atlanta, May 1996*, p. 1323.
12. P. E. Merilees, The pseudospectral approximation applied to the shallow water equations on the sphere, *Atmosphere* **11**(1), 13 (1973).

13. P. E. Merilees, Numerical experiments with the pseudospectral method in spherical coordinates, *Atmosphere* **12**(3), 77 (1974).
14. S. A. Orszag, Fourier series on spheres, *Monthly Weather Rev.* **102**, 56 (1974).
15. M. Rančić, R. J. Purser, and F. Mesinger, A global shallow water model using an expanded spherical cube: Gnomonic versus conformal coordinates, *Quart. J. R. Meterological Soc.* **122**(532), 959 (1996).
16. H. Ritchie, Application of the semi-Lagrangian method to a spectral model of the shallow water equations, *Monthly Weather Rev.* **116**, 1587 (1988).
17. A. J. Robert, The integration of a low order spectral form of the primitive meteorological equations, *J. Meteorological Soc. Japan* **44**(5), 237 (1966).
18. C. Ronchi, R. Iacono, and P. S. Paolucci, The "cubed sphere": A new method for the solution of partial differential differential equations in spherical geometry, *J. Comput. Phys.* **124**(1), 93 (1996).
19. P. N. Swarztrauber, The vector harmonic transform method for solving partial differential equations in spherical geometry, *Monthly Weather Rev.* **121**(12), 3415 (1993).
20. P. N. Swarztrauber, Spectral transform methods for solving the shallow-water equations on the sphere, *Monthly Weather Rev.* **124**, 730 (1996).
21. P. N. Swarztrauber, On the spectral approximation of discrete scalar and vector functions on the sphere, *SIAM J. Numer. Anal.* **16**(6), 934 (1979).
22. P. N. Swarztrauber, D. L. Williamson, and J. B. Drake, The cartesian method for solving partial differential equations in spherical geometry, *Dynam. Atmospheres Oceans* **27** (1997).
23. M. Taylor, J. Tribbia, and M. Iskandarani, The spectral element method for the shallow water equations on the sphere, *J. Comput. Phys.* **130**, 92 (1997).
24. C. Temperton, Algorithms for the solution of cyclic tridiagonal systems, *J. Comput. Phys.* **19**, 317 (1975).
25. C. Temperton, On scalar and vector transform methods for global spectral models, *Monthly Weather Rev.* **119**, 1303 (1991).
26. L. Umscheid and M. Sankar-Rao, Further tests of a grid system for global numerical prediction, *Monthly Weather Rev.* **99**(9), 686 (1971).
27. D. L. Williamson, J. B. Drake, J. J. Hack, R. Jakob, and P. N. Swarztrauber, A standard test set for numerical approximations to the shallow water equations in spherical geometry, *J. Comput. Phys.* **102**(1), 211 (1992).
28. N. Yarvin and V. Rokhlin, *A Generalized One-Dimensional Fast Multipole Method with Application to Filtering of Spherical Harmonics*, Technical Report, Research Report 1142, Yale Computer Science Department, 1998.